Neuromorphometric characterization with shape functionals

Marconi Soares Barbosa* and Luciano da Fontoura Costa†
Cybernetic Vision Research Group, GII-IFSC, Universidade de São Paulo, São Carlos, São Paulo, Caixa Postal 369, 13560-970, Brazil

Esmerindo de Sousa Bernardes‡
Departamento de Física e Ciência dos Materiais, Universidade de São Paulo, São Carlos, São Paulo, Caixa Postal 369, 13560-970, Brazil

(Received 6 October 2002; published 23 June 2003)

This work presents a procedure to extract morphological information from neuronal cells based on the variation of shape functionals as the cell geometry undergoes a dilation through a wide interval of spatial scales. The targeted shapes are α and β cat retinal ganglion cells, which are characterized by different ranges of dendritic field diameter. Image functionals are expected to act as descriptors of the shape, gathering relevant geometric and topological features of the complex cell form. We present a comparative study of classification performance of additive shape descriptors, namely, Minkowski functionals, and the nonadditive multiscale fractal. We found that the proposed measures perform efficiently the task of identifying the two main classes α and β based solely on scale invariant information, while also providing intraclass morphological assessment.

DOI: 10.1103/PhysRevE.67.061910 PACS number(s): 87.80.Pa, 87.19.La

I. INTRODUCTION

Many natural phenomena are defined or influenced by the geometrical properties of the involved elements, and vice versa. Examples of such a shape-function relationship include the chemical properties of proteins, the aerodynamic efficiency of wings, and the oxygen exchanges through elaborated bronchic structures. A close relationship between geometry and function provides strong motivation for the geometrical analysis of natural objects. Yet, the state of the art of geometrical characterization, an area sometimes called morphometry or morphology, remains in a relatively incipient stage where several competing, and often divergent, approaches coexist. While powerful methods have been used in physics to express relevant geometrical properties, often including differential measurements such as curvature, the situation remains particularly challenging in biology.

The relationship between neuronal shape and function has attracted increasing attention due to its far reaching implications for basic neuroscience and medical applications. Neuron morphology has the special characteristic, that it evolves during the developmental stage of the cell, being influenced by its molecular environment and the history of synaptic activity [1]. The mature neuronal shape, together with its membrane electrical properties, determines the electric conductance of the cell [2] and accounts for part of its electrophysiological characteristics, such as firing patterns and computational abilities [3–6]. Software packages, such as NEURON, are available for modeling neuronal activity with basis on cable theory [7], which can be useful for an analysis of real or virtual neurons [8–10]. At the same time, neuronal shape can vary for different tissues, depending on a number of extracellular factors [1,11]. Ultimately, it determines the patterns of connectivity and, consequently, the overall network computational abilities. On the application side, tasks such as automated morphological characterization of neuronal shape and the diagnosis of abnormalities deserve further investigation.

While the use of morphological tools was severely constrained until recently by the cost of the relatively sophisticated systems needed to process images and geometry, the continuing advances in computer software and hardware have paved the way for an ever widening range of possible applications. Consequently, more effective morphological concepts and methods have been developed and reported in the literature, including the use of differential geometry concepts such as multiscale curvature and bending energy [12–14], methods from mathematical morphology such as skeletonization [15,16], as well as the recently reported framework known as integral-geometry morphological image analysis (MIA) [17–19]. The latter approach involves the use of additive shape functionals, i.e., mappings that take shapes to single scalar values, in terms of a parameter usually related to the spatial scale or time. As far as neuroscience is concerned, the contour of a neuronal cell has been shown to possess a fractal structure [20] and its multiscale fractal dimension has been used to characterize different morphological classes of neuronal cells [21].

Primarily motivated by the possibility of applying the methodology proposed in Refs. [18,19] as a novel and potentially useful tool for addressing the problem of neuronal shape characterization and classification, the present work also provides an assessment of those measures considering a database of real biological data, namely, camera lucida images of cat ganglion neuronal cells. In order to provide a comparative reference, the multiscale fractal dimension [21], itself a shape functional, is also considered as a measure for shape characterization.

Integral geometry provides an adequate mathematical framework for morphological image analysis, having a core of useful theorems and formulaes, which in some cases leads

*Electronic address: marconi@if.sc.usp.br
†Electronic address: luciano@if.sc.usp.br
‡Electronic address: sousa@if.sc.usp.br

to analytical results for averages of image functionals [17] while also being quite efficient to implement computationally [18]. Here, the class of functionals involved is restricted to additive, motion invariant, and continuous, called Minkowski functionals. These functionals are related to usual geometric quantities, for instance, in the Euclidean plane, to area, perimeter, and connectivity or the Euler number, which expresses the number of holes in a connected pattern such as the image of a neuronal cell.

In order to describe geometrically one object, a set of measures (functionals) is taken and the behavior of these measures is monitored, as some control parameter is varied. In this work, we compute additive functionals in the plane as the contour of a neuronal cell image is inflated by a parallel set dilation of radius r, the control parameter. The nonadditive multiscale fractal dimension is derived from one of these computed additive functionals, at each radius of dilation, giving important [22] complementary information.

This paper starts by presenting the adopted methodology, the considered shape functionals, and the statistical procedure for cell identification. The results, which are presented subsequently, clearly indicate that the proposed measures are efficient for distinguishing morphologically the two functional classes α and β as well as revealing a strong morphological coherence in one of the classes.

II. METHODOLOGY

A. Additive shape functionals

The morphological characterization in Euclidean plane by means of shape functionals explores simple properties of convex sets. For these basic geometric objects, such as a triangle or an ellipse, we may evaluate a change in area while the object undergoes a morphological dilation with the knowledge of its initial geometry. For example, the change in area of a convex body K, after a parallel set dilation using a two dimensional (2D) ball of radius r, can be expressed as

$$A(K_r)=A(K)+U(K)r+\pi r^2, \tag{1}$$

where $A(K)$ and $U(K)$ stand for the initial area and perimeter of the object K, and r is the dilation parameter. The process of taking parallel sets generalizes naturally to higher dimensions, while the change in hypervolume preserves the general form (1) and is given by the Steiner formula

$$v^d(K_r)=\sum_{\nu=0}^{d}\binom{d}{\nu}W_\nu^{(d)}(K)r^\nu, \tag{2}$$

where the coefficients $W_\nu^{(d)}$ are referred to as *quermassintegrals* or Minkowski functionals, [19]. These functionals, as a generalization of known geometric quantities, are additive, motion invariant, and continuous. Moreover, a theorem by Hadwiger [17,19] states that these functionals form a complete set of measures, with the above properties, on the set of convex bodies

$$\phi(K)=\sum_{j=0}^{d} c_j W_j^{(d)}(K). \tag{3}$$

Notwithstanding, the change of any, additive, motion invariant, and continuous, functional can be expressed, using a generalized Steiner formula [17,23], in terms of the initial geometric information

$$\phi(K_r)=\sum_{j=0}^{d}\sum_{k=0}^{d-j} c_j\binom{d-j}{k}W_{k+j}^{(d)}(K)r^k. \tag{4}$$

The notion of connectivity number or Euler characteristic χ is central in establishing the aforementioned properties of Minkowski functionals. The usual definition of the connectivity from algebraic topology in two dimensions is the difference between the number of connected n_c components and the number of holes n_h,

$$\chi(K)=n_c-n_h, \tag{5}$$

while in three dimensions the distinction should be made between two kinds of holes, namely, cavities n_{hc} and handles (tunnels) n_{hh}

$$\chi(K)=n_c-n_{hh}+n_{hc}. \tag{6}$$

The integral geometry provides an equivalent definition for connectivity number of a convex set K, which is given by

$$\chi(K)=\begin{cases}1, & K\neq\varnothing\\ 0, & K=\varnothing.\end{cases} \tag{7}$$

Of great importance is its property of additivity

$$\begin{aligned}\chi(A)&=\chi(\cup_{i=1}^{l}K_i)\\ &=\sum_i \chi(K_i)-\sum_{i<j}\chi(K_i\cap K_j)\\ &\quad+\cdots+(-1)^{l+1}\chi(K_1\cap\cdots\cap K_l).\end{aligned} \tag{8}$$

Additivity and motion invariance are inherited by the Minkowski functionals as these are related to the connectivity number by the following formulas

$$\begin{aligned}W_\nu^{(d)}(A)&=\int_{\mathcal{G}}\chi(A\cap E_\nu)d\mu E_\nu, \quad \nu=0,\ldots,d-1\\ W_d^{(d)}(A)&=\omega_d\chi(A), \quad \omega_d=\pi^{d/2}/\Gamma(1+d/2).\end{aligned} \tag{9}$$

In the above expression, E_ν stands for a ν-dimensional plane in R^d. The integral is to be taken for all positions, induced by isometries $\mathcal{G}$, of E_ν weighted by $d\mu(E_\nu)$, the kinematical density which is in turn related to the Haar measure on the group of motions $\mathcal{G}$, see Refs. [17,19,23].

To sum up, the Minkowski functionals $W_\nu^{(d)}(A)$, as a generalization of the usual procedure for volume determination, count the number of possible intersections of a ν-dimensional plane with the domain A.

If one is to take advantage of the above additivity property, all intersections in Eq. (8) must be taken into account. When working on a lattice, there is a more expedient route, exploring the discrete nature of the images and the additivity

TABLE I. Minkowski functionals of elementary open bodies which compose a pixel K.

m	$\check{N}_m$	$W_0^{(2)}=A(\check{N}_m)$	$W_1^{(2)}=\frac{1}{2}U(\check{N}_m)$	$W_2^{(2)}=\pi\chi(\check{N}_m)$
0	$\check{P}$	0	0	π
1	$\check{L}$	0	a	$-\pi$
2	$\check{Q}$	a^2	$-2a$	π

of the Minkowski functionals, which consists of a decomposition of the 2D body A into a disjoint collection of interior bodies, open edges, and vertices. Following the usual nomenclature, we denote the interior of a set A by $\check{A}=A/\partial A$. For an open interior of an n-dimensional body embedded in a d-dimensional Euclidean space, there is the following expression for the Minkowski functionals [19]:

$$W_\nu^{(d)}(\check{A})=(-1)^{d+n+\nu}W_\nu^{(d)}(A), \quad \nu=0,\ldots,d. \tag{10}$$

We may then apply additivity and the lack of connectivity of open sets on the lattice to determine the functionals for the body as a whole:

$$W_\nu^{(d)}(\mathcal{P})=\sum_m W_\nu^{(d)}(\check{N}_m)n_m(\mathcal{P}), \quad \nu=0,\ldots,d. \tag{11}$$

Here $n_m(\mathcal{P})$ stands for the number of building elements of each type m occurring in the pattern $\mathcal{P}$. For a two-dimensional space, which is our interest for the present neuron images, we display in Table I the value of Minkowski functionals for the building elements on a square lattice of pixels and their direct relation to familiar geometric quantities on the plane. Using the information presented in Table I and Eq. (11), we have

$$A(\mathcal{P})=n_2, \quad U(\mathcal{P})=-4n_2+2n_1, \quad \chi(\mathcal{P})=n_2-n_1+n_0. \tag{12}$$

So, the procedure of calculating Minkowski functionals of a pattern $\mathcal{P}$ has been reduced to the proper counting of the number of elementary bodies of each type that compose a pixel (squares, edges, and vertices) involved in the make up of $\mathcal{P}$.

In Sec. III we describe typical results for the evaluation of the above presented additive functionals using an actual neuron image. The procedure involves the implementation of, first, an algorithm for the proper parallel set dilation throughout all permitted radii on the square lattice and, second, of an algorithm for the calculation of Minkowski functionals by counting disjoint building elements based on the formulas (12). An efficient routine for undertaking the latter is described in detail in Refs. [18,19].

B. Multiscale fractal dimension

As an example of a related nonadditive functional, we add to the previous measures the multiscale fractal, an approach which has been applied successfully to neuromorphometry [22]. The notion of multiscale fractal dimension refers to a quantitative characterization of complexity and the degree of self-similarity at distinct spatial scales, see Refs. [21,22]. Intuitively, the fractal dimension indicates how much the curve extends itself throughout the space. As a consequence, more intricate curves will cover the surround space more effectively and will display a higher fractal dimension. This quantity is calculated via the derivative of the logarithm of the changing interior area as the neuron cell image undergoes a dilation. As such it is immediately derivable from the first additive functional (area) in a pixel based approach as opposed to a curvature approach, see Ref. [21].

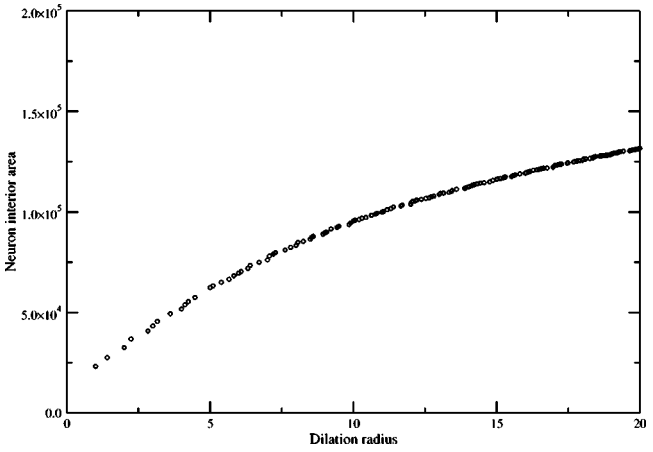

FIG. 1. Area (in pixels) as a function of the scale radius (in pixels) for a typical α neuronal cell given in Fig. 6. Subtle information in this graphic is revealed only through the multi-scale fractal dimension.

C. Implementation

We have conducted the evaluation of the functionals described above on a 800 MHz ordinary personal computer running Linux. Both the algorithm for exact dilations on the square lattice, according to Ref. [24], and the pixel based algorithm for the estimation of the Minkowski functionals

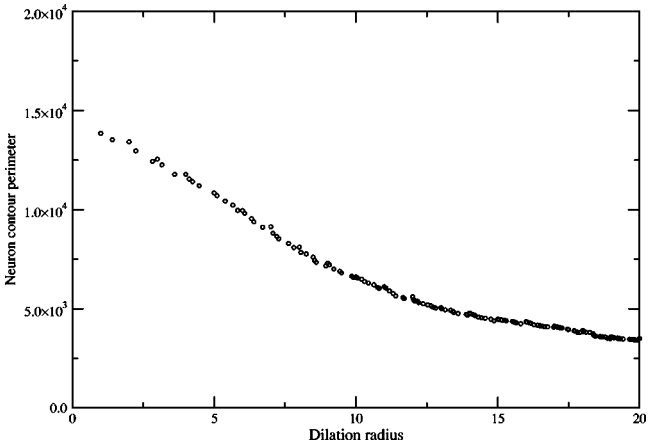

FIG. 2. Perimeter (in pixels) as a function of the scale radius (in pixels) for the α neuronal cell of Fig. 6. Note the expected initial decline and a visible fine structure associated with the disappearing and less frequently appearing holes.

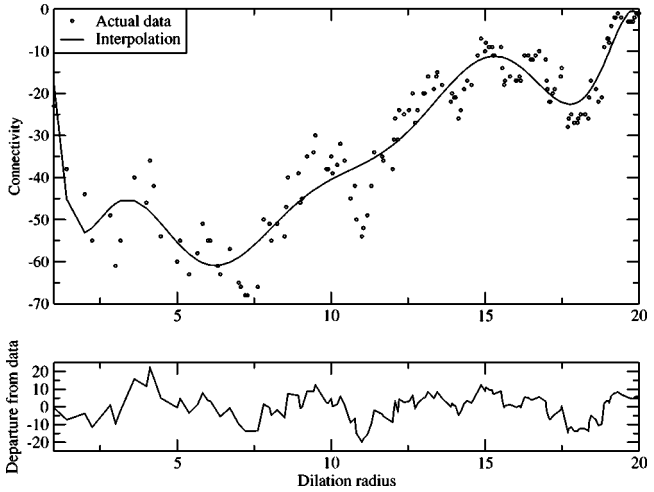

FIG. 3. Connectivity and the difference between data and interpolation for the typical α neuronal cell, Fig. 6, as a function of parallel set dilation radius (in pixels).

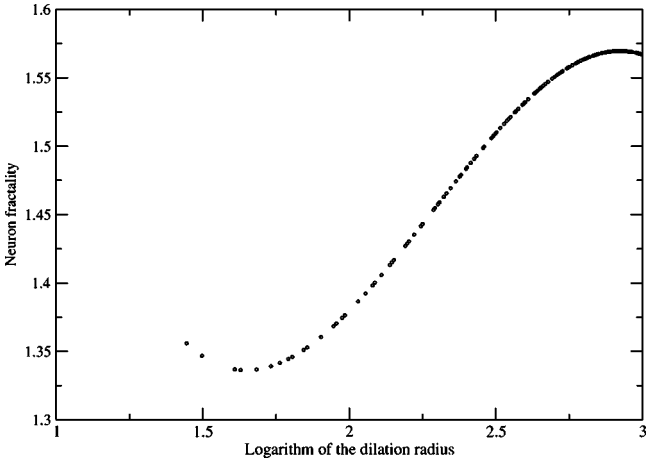

FIG. 5. Multiscale fractality of a neuronal type α cell. This attribute is obtained from the area functional and shows the fine structure that is not revealed by this functional alone. Dilation radius in pixels.

[19] were implemented in SCILAB-2.6. It took $\approx$40 s to calculate the functionals for each dilation radius.

III. RESULTS

We start by describing a measure that is perhaps the simplest one, but holds important information not only on its own but also through relation with the multiscalar fractal dimension described in Sec. II B. In Fig. 1, we show the typical monotonically increasing curve of the interior area of a neuron cell as its contour is inflated by a parallel set procedure. To capture the gross structure of this measure we calculate the area under curve sum^a and, in a size independent manner, radius $R^a_{1/2}$ at which the area below this curve reaches half of its value at the end of dilation. The fine structure is given by its standard deviation std^a.

In Fig. 2, we show a typical curve of the perimeter of the evolving frontier of the neuron cell as the contour is inflated by a parallel set procedure. It is important to observe that this measure is affected by errors introduced by the discrete nature of the lattice of pixels and the low resolution of the original image, which become more acute in β cells because of their reduced size. Nonetheless, this effect tends to be less important after the tenth radius or so. To capture the gross structure of this measure, we calculate the area under curve sum^p and the size independent radius $R^p_{1/2}$ at which the area below this curve reaches half of its overall value. The fine structure is given simply by the standard deviation of the data, std^p.

In contrast to the preceding measure, the connectivity or the Euler number of the neuron shape as it undergoes the dilation processes is independent of the resolution of the image. It is a measure restricted to the topology of the shape counting essentially the number of holes at each radius of dilation, no matter the holes are perfectly round or not. The

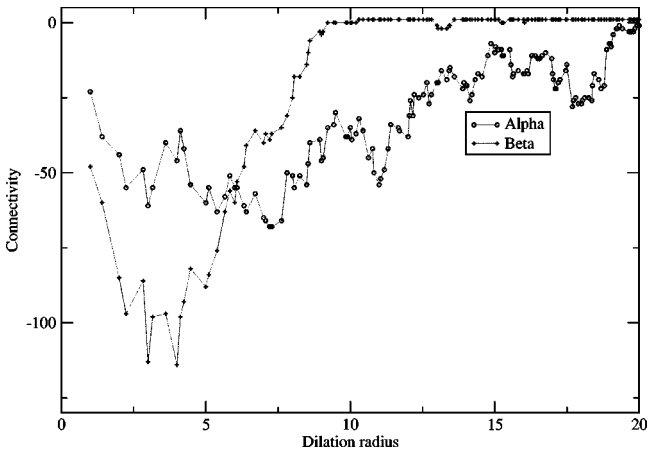

FIG. 4. Comparison between the connectivities of typical α and β cells showing a different range (in pixels) of complexity for the two class of neurons.

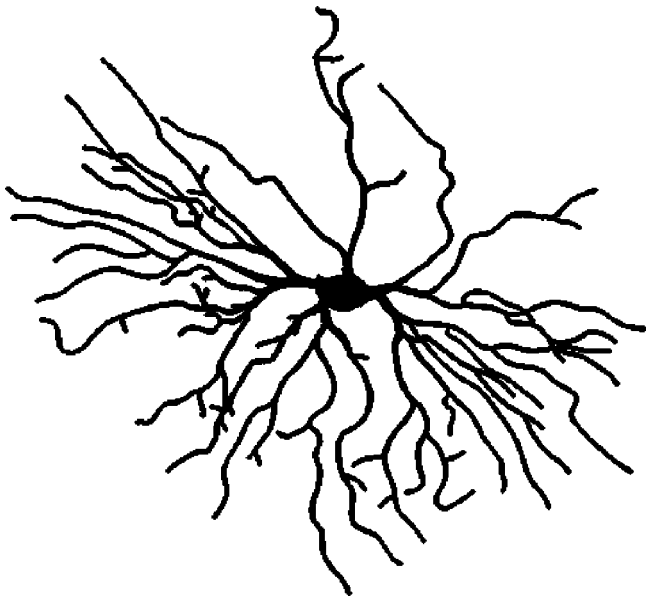

FIG. 6. Initial neuron image. (See Ref. [26].)

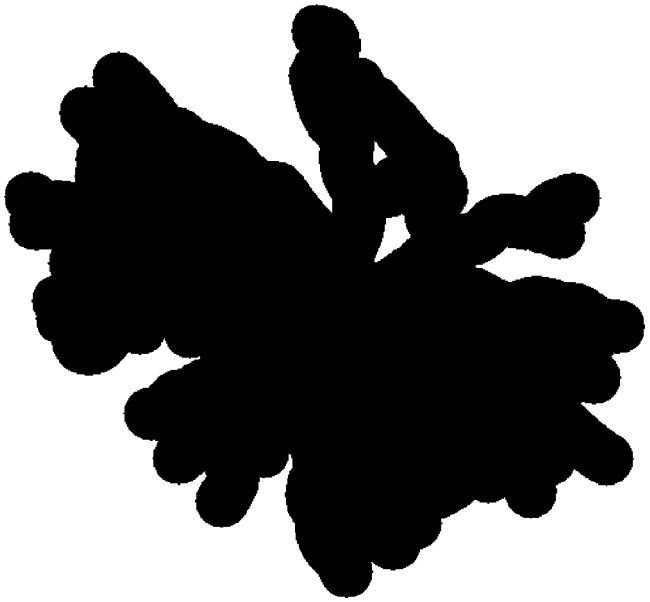

FIG. 7. The same neuron image after the parallel set dilation.

alterations of connectivity are subtle from step to step, which is reflected by the complex distribution of cusps in Fig. 3. The vast amplitude of scale for which there is an abrupt change of connectivity is a measure of complexity of this type of cell. Figure 4 shows the particular behavior of the connectivity, for samples from the two classes, as the cell shape undergoes a dilation. We take the gross information of this measure by extracting the area under the interpolated curve $\mathsf{sum}_{\mathsf{interp}}$ and by a monotonicity index given by

$$i_s = \frac{s}{s+d+p}, \tag{13}$$

where $s, d,$ and p count, respectively, the number of times the curve increases, decreases, and reaches a plateau. This index characterizes a perfect monotonically increasing curve when its value is 1 and reaching its minimum value for a curve of high variability. This measure is designed specially to explore the multiscale nature of the neuronal complexity. The finer structure is captured solely by the standard deviation $\mathsf{std}_{\mathsf{diff}}$ of the difference between the interpolated curve and the original data.

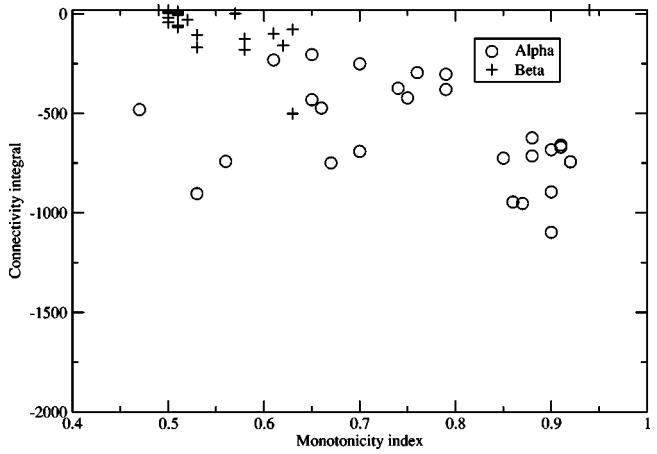

FIG. 9. The feature space based on the index of monotonicity and the integral of the connectivity (interpolated) curve, for both α and β cells showing a strong clustering of the β neuron class and a much dispersed α class.

As a measure of complexity, the multiscale fractal dimension has been experimentally found to be related to the connectivity of a shape. Although this relationship is not straightforward, there might be a correlation between these measures as commented below. For this image functional, we evaluate the maximum fractal dimension, the mean fractality, and the standard deviation, respectively, max, mean, and std^f. A typical curve for the multiscale dimension is shown in Fig. 5 for the same neuron appearing in Figs. 6 and 7.

Among all the considered measurements, we found a good separation of α and β type cells for the feature space defined by the perimeter half integral radius $\mathsf{R}^p_{1/2}$, and the standard deviation for the fine structure of connectivity, $\mathsf{std}_{\mathsf{diff}}$. Figure 8 shows the obtained α and β clusterings with both classes exhibiting similar dispersion. Another good result for morphological characterization was obtained for the

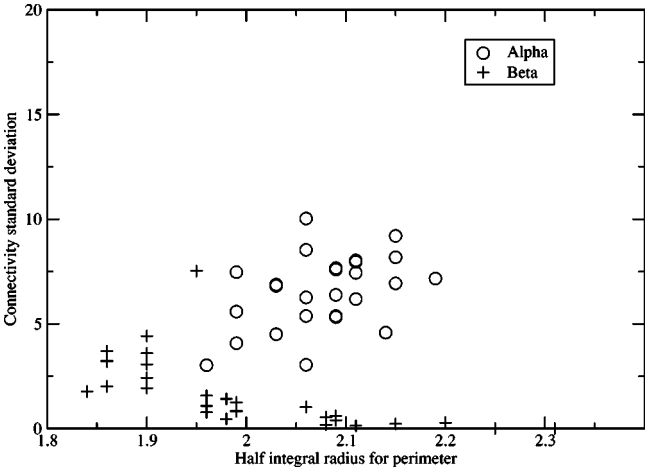

FIG. 8. Clustering of α and β cells based on $R^p_{1/2}$ (in pixels) and connectivity measures.

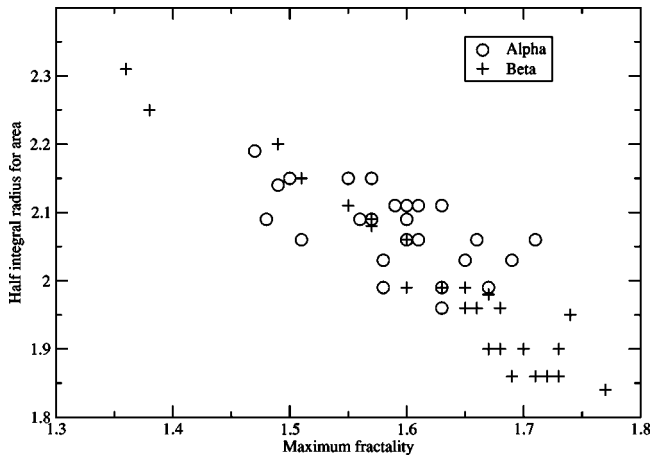

FIG. 10. A not decisive feature space: related measures with high (anti-)correlation. Half integral radius in pixels.

TABLE II. Correlation coefficients for the set of the measures extracted from area, perimeter, connectivity, and fractality: standard deviations ($std^{a,p,f}$, std_{diff}), integrals ($sum^{a,p}$, sum_{interp}), half radii ($R^{a,p}_{1/2}$), the monotonicity index (i_s), mean value (mean), and max value (max). Bold face for absolute values of correlation above 0.5.

	Area			Perimeter			Connectivity			Fractality		
	std^a	sum^a	$R^a_{1/2}$	std^p	sum^p	$R^p_{1/2}$	std_{diff}	sum_{interp}	i_s	std^f	max	mean
std^a	1											
sum^a	**0.96**	1										
$R^a_{1/2}$	**0.51**	0.41	1									
std^p	**0.86**	**0.96**	0.33	1								
sum^p	**0.97**	**0.99**	0.45	**0.94**	1							
$R^p_{1/2}$	0.13	0.01	**0.78**	−0.05	0.03	1						
std_{diff}	**0.78**	**0.88**	0.15	**0.90**	**0.87**	−0.27	1					
sum_{interp}	−0.79	−0.92	−0.22	−0.98	−0.90	0.17	−0.92	1				
i_s	0.33	0.44	0.34	**0.52**	0.44	−0.02	0.43	−0.57	1			
std^f	−0.24	−0.27	0.16	−0.19	−0.27	**0.58**	−0.40	0.27	−0.34	1		
max	−0.34	−0.18	−0.86	−0.01	−0.23	−0.65	0.05	−0.07	−0.22	0.10	1	
mean	0.14	0.30	−0.63	0.39	0.26	−0.88	**0.55**	−0.49	0.22	−0.64	0.63	1

connectivity or the Euler number of the cell shape. A feature space involving the index of monotonicity and the integral of the interpolated connectivity curve is presented in Fig. 9. More efficient than the former in separating the two classes, these measures produce a well-localized clustering of β cells characterizing its geometrical intricacies. This result suggests that α class is indeed a more homogeneous category, while the β class may have a morphological subclass structure.

Table II shows the correlation coefficients for the 12 measurements considered in this work. Of special interest is the correlation between fractality and connectivity, measures that have experimentally been found to represent complementary but not redundant measures of complexity. Figure 10 shows a combination of two measures to form a feature space, which in this case shows a poor separation of classes, this is in accordance with the high anti-correlation of the involved measures, presented in Table II. Unusually high correlation appears between some measures, notably as occurring between area and perimeter, suggesting a specific tendency that seems to be particular to the type of data (neurons) and not a general rule.

IV. CONCLUSIONS

The use of additive shape functionals has been recently considered for the characterization of the geometrical properties of several physical objects [17,19]. The current paper explored the use of a representative set of such functionals, namely, the area, perimeter, and connectivity, for the characterization of neural shapes represented in terms of a whole set of parallel expansions. The multiscale fractal dimension, a nonadditive shape functional, was also considered as a standard for comparison.

All the adopted shape functionals consist of functions of the dilating radius of each parallel body. For the sake of efficiency, the following compact subset of global features was selected: the area under the functionals, the value of radius where the area reaches its half-value, the standard deviation of the functionals, as well as proposed measurements expressing the monotonicity of the functionals and the decomposition of the connectivity functional in terms of a low and high variation signals.

All two-by-two combinations of these measures were investigated visually in order to identify the combinations of features leading to more pronounced separations between the two classes of considered neural cells, namely, cat retinal ganglion cells of type α and β. The coefficients of correlation of each pair of measures were also estimated and analyzed, indicating decorrelation between several of the considered features. The obtained results confirmed a differentiated potential of each measurement for neural cell clustering, with the features derived from the connectivity functional accounting for the best separation between classes. However, further investigation and comparison to more established and recent methods (such as in Ref. [25]) based explicitly on dendritic morphology will be necessary to reveal the best realization of the different methodology proposed in this paper. The biological implications of such results are that the two type of cells differ in the distribution of holes (defined by the respective dendritic arborizations) for different spatial scales. The obtained clusters indicated that the α cells exhibit less uniform geometrical properties than the β, suggesting the existence of morphological subclasses.

ACKNOWLEDGMENTS

The authors are grateful to FAPESP (Grant Nos. 02/02504-01, 99/12765-2, and 96/05497-3) and to CNPQ (Grant No. 301422/92-3) for financial support.

[1] K.L. Whitford, P. Dijkhuizen, F. Polleux, and A. Ghosh, Annu. Rev. Neurosci. **25**, 127 (2002).
[2] C. Koch and I. Segev, Nat. Neurosci. **3**, 1171 (2000).
[3] Y. Fukuda, C.F. Hsiao, M. Watanabe, and H. Ito, J. Neurophysiol. **52**, 999 (1984).
[4] H.G. Krapp, B. Hengstenberg, and R. Hengstenberg, J. Neurophysiol. **79**, 1902 (1998).
[5] A. van Ooyen, J. Duijnhouwer, M.W.H. Remme, and J. van Pelt, Network Comput. Neural Syst. **13**, 311 (2002).
[6] H. Wassle, B.B. Boycott, and R.B. Illing, Philos. Trans. R. Soc. London **212**, 177 (1981).
[7] W. Rall, in *Handbook of Physiology*, edited by E.R. Kandel (American Physiological Society, Bethesda, MD, 1977), Vol. 1, pp. 39–97.
[8] G.A. Ascoli, Network Comput. Neural Syst. **13**, 247 (2002).
[9] R.C. Coelho and L. da F. Costa, in *Third IEEE International Conference on Engineering of Complex Sytems, Villa Olmo, Como, Italy*, edited by Bob Werner (IEEE Computer Society, Los Alamitos, CA, 1997), pp. 223–228.
[10] G. Ascoli, in *Computational Neuroanatomy: Principles and Methods*, edited by G. Ascoli (Humana Press, Totowa, NJ, 2002), Chap. 3, pp. 49–70.
[11] E.R. Kandel and J.H. Schwartz, *Principles of Neuroscience* (Elsevier, New York, 1985).
[12] R.M. Cesar and L. da F. Costa, Rev. Sci. Instrum. **68**, 2177 (1997).
[13] R.M. Cesar and L. da F. Costa, Biol. Cybern. **79**, 347 (1998).
[14] L. da F. Costa and T.J. Velte, J. Comp. Neurol. **404**, 33 (1999).
[15] L. da F. Costa, Real-Time Imag. **6**, 415 (2000).
[16] A.X. Falcao, L. da F. Costa, and B.S. Cunha, Pattern Recogn. **7**, 1571 (2002).
[17] K.R. Mecke, Int. J. Mod. Phys. A **12**, 861 (1998).
[18] K. Michelsen and H. de Raedt, Comput. Phys. Commun. **132**, 94 (2000).
[19] K. Michelsen and H. de Raedt, Phys. Rep. **347**, 461 (2001).
[20] K. Morigiwa, M. Tauchi, and Y. Fukuda, Neurosci. Res. (NY) **10**, S131 (1989).
[21] L. da F Costa, E.T.M. Manoel, F. Faucereau, J. Chelly, J. van Pelt, and G. Ramakers, Network Comput. Neural Syst. **13**, 283 (2002).
[22] L. da F Costa, E.T.M. Manoel, and A.G. Campos, *An Integrated Approach to Shape Analysis: Results and Perspectives* (Cépaduès-Éditions, Toulouse, 2001), Vol. T1, pp. 23–34.
[23] L.A. Santaló, *Integral Geometry and Geometric Probability* (Addison-Wesley, Reading, MA, 1976).
[24] L. da F. Costa and E.T.M. Manoel, Opt. Eng. **40**, 1752 (2001).
[25] A. Mizrahi, E. Ben-Ner, M.J. Katz, K. Kenden, J.G. Glusman, and F. Libersat, J. Comp. Neurol. **422(3)**, 415 (2000).
[26] Reprinted with permission from B.B. Boycott and H. Wässle, J. Physiol. (London) **240**, 402 (1974).